Molecular Dynamics Simulation of Atactic Polystyrene. 3. Short Range Order

Ryong-Joon Roe,* M. Mondello,† Hidemine Furuya,‡ and Hyung-Jin Yang§

Department of Materials Science and Engineering, University of Cincinnati, Cincinnati, Ohio 45221

Received September 2, 1994; Revised Manuscript Received January 25, 1995®

ABSTRACT: A molecular dynamics simulation of bulk atactic polystyrene was performed, and the result was analyzed in detail to evaluate the *intra*molecular and *inter*molecular short range orders present. In this work the analysis was performed only on the results obtained from the united atom model, since, as was shown in the previous two publications, it gives much better agreement with experiment than the all atom model. Most of the study was performed with a system containing a single 80-monomer molecule, but some study was also made with a system containing two 40-monomer molecules. The short range order was examined by evaluating the radial distribution functions and orientational order parameters of pairs of aliphatic backbone segments and of phenyl group centers. In the case of *intra*molecular phenyl pairs, these quantities were evaluated individually according to the monomeric distance along the chain by which the two phenyls are separated. The conformation of the molecule was examined by evaluating the population distribution of backbone bond torsional angles in meso and racemic diads. The result resembles the conformational energy maps previously prepared by others, but some differences were also noted. The most prominent feature in the *inter*molecular correlation is the strong tendency for the phenyl groups to have a separation distance of about 6 Å. A detailed analysis was given to define the relative orientation that the pair of phenyls adopt at this separation. *Inter*molecular pairs of backbone segments were found to be oriented mostly randomly at separation distances larger than 6 Å.

Introduction

Much progress has been made in recent years in the experimental, theoretical, and computer simulation studies of small molecule liquids,[1,2] and a fair degree of understanding of the short range order present in these simple liquids is now available. For polymer scientists, however, further questions remain concerning whether the long chain nature of polymer molecules produces orders beyond those found in simple liquids. The subject of the degree of short range order present in bulk, amorphous polymers has attracted the interest of many workers over the years. Although the claims for the presence of some organized regions of size ~100 Å, called nodules, bundles, meander arrays, etc.,[3–5] have now largely subsided, alternative descriptions specifying the nature and degrees of order present have not been readily forthcoming. In this work we perform a molecular dynamics simulation of bulk, atactic polystyrene and analyze its results in detail to examine the short range order present. Polystyrene is the most typical of amorphous, glassy polymers and has been widely studied with a variety of experimental techniques. Polystyrene poses a particular challenge in that, although it has been repeatedly studied by means of X-ray and neutron diffraction,[6–18] the diffraction patterns observed could not easily be interpreted on the basis of structural models. In particular, the so-called "polymerization peak", conspicuous in the X-ray scattering pattern at an angle smaller than the main amorphous peak, could not be reproduced in calculations based on the structure of single chains known, for example, from the rotational isomeric states model approach. Efforts were also made to interpret the amorphous structure by performing Fourier transformation of the experimental scattering curves, but little additional insight could be gained because of the resolution limitation inherent to radial distribution functions thus derived.

Computers have now become powerful enough to allow simulation of realistic models of bulk amorphous polymers of a sufficient volume suitable for investigation of short range order. Of course in such an endeavor the most important point to make sure is that the model in fact reproduces features of interest in the real system sufficiently faithfully. As described in detail in the previous two publications (hereafter referred to as part 1[19] and part 2[20]), we have performed a molecular dynamics simulation of bulk atactic polystyrene in the united atom model and all atom model. In part 1 X-ray scattering curves were calculated from the MD results and comparison was made with experimental curves available in the literature. In part 2 neutron scattering curves were calculated from the MD results for selectively deuterated polystyrenes and were compared with our own experimental measurements obtained by the technique of neutron spin polarization analysis,[21–23] which permits separation of incoherent from coherent scattering. In both cases the united atom model gave a fairly satisfactory agreement. Although some minor discrepancies remained between experiment and simulation, these were largely within the uncertainties of the experimental data themselves, which were estimated, in the case of X-ray data, from discrepancies between different sets of published data and, in the case of neutron data, from the assessment of statistical errors. The most essential features, such as the locations and relative sizes of all scattering peaks including the polymerization peak, were correctly reproduced. The polymerization peak is known[10,24] to gain its height at higher temperatures, and the model correctly reproduces[25] such a temperature dependence as well. Furthermore, the thermal expansion coefficients above and below T_g and the glass transition temperature itself

† Present address: Exxon Research and Engineering Co., Annandale, NJ 08801.

‡ Present address: Department of Polymer Chemistry, Tokyo Institute of Technology, Meguro-ku, Tokyo, Japan.

§ Present address: Department of Physics, Jochiwon Campus, Korea University, Korea.

® Abstract published in *Advance ACS Abstracts,* March 1, 1995.

0024-9297/95/2228-2807$09.00/0

obtained[25] from the model also agree well with experiment. Thus we can place some confidence in the detailed short range structure that is derived from the model as is described below.

In contrast, with the all atom model we were unable to produce results with equally satisfactory agreement with experiment, especially in the part of the scattering curve that includes the polymerization and main amorphous peaks. Agreement in these scattering angle regions are essential if the structure in the distance scale relevant to the so-called short range order is to be faithfully represented. Inclusion of partial electric charges and electrostatic interactions, as available in one of the commercial molecular modeling software programs, did not remedy the problem. We therefore make use of only the united atom model in this work and analyze the atomic coordinates obtained from it to evaluate the detailed short range structure in polystyrene.

Model and Method of Calculations

The model and the method of computation were described in detail in the previous two publications.[19,20] Although both the united atom model and all atom model were used, in this work we analyze only the results obtained from the united atom model. In both models the bond lengths are kept fixed, and the phenyl group is represented by a rigid planar hexagon with six pseudocarbons at the six corners. Part 1 lists all the force constants used, including those for the bond angle bending, torsional rotation around the C−C bonds in the chain backbone, and the Lennard-Jones nonbonded interactions acting on atomic pairs separated by more than two bonds. Most of the results in this work were obtained with a system containing a single atactic polystyrene molecule consisting of 80 monomer units and its images created by the periodic boundary conditions. The cubic MD cell is of edge length 23.79 Å, so that the mass density is equal to 1.028 g/cm^3, closely approximating the experimental bulk density. Additionally, some limited amount of study was also made with a system containing two polystyrene molecules of 40 monomers each and their images. This additional system was studied as a means of checking how different methods of separating *intra-* from *inter*molecular correlations affect the results, as will be discussed below.

MD runs were made at 500 K from three independent starting configurations. Molecules in configurations A and B have the same stereochemical sequence of monomers, but their chain conformations are very different between the two as a result of the diverse temperature-density histories to which they were subjected before the equilibration. The density of 1.028 g/cm^3 corresponds to that of glassy polystyrene, and therefore, even though 500 K is nominally above the glass transition temperature of polystyrene, our simulated system is apparently still in the glassy state, and the chain conformations did not relax appreciably during the 500 ps runs. The molecule in configuration C has an entirely different stereochemical sequence generated by an independent Bernoulli run. The number of meso diads in configurations A and B is 27 out of 78 (35%) and that in configuration C is 29 out of 78 (37%), in comparison to the ordinary atactic polystyrene which is said to contain approximately 40% meso diads.[26] The starting configurations for the second system containing two shorter molecules were derived by severing the covalent link between the 40th and 41st monomers in the longer molecule system before a further equilibration. With both systems the atomic coordinates were recorded at the interval of 1 ps during the MD runs of 500 ps duration. The short range structures evaluated from these sets of atomic coordinates were then combined and averaged over the three configurations before being reported in this work. The structures derived from the individual configurations differ insignificantly among them and would not have affected the main conclusions drawn even if individual results were displayed separately.

The root-mean-square end-to-end distances of the molecules evaluated during the 500 ps are 24.7, 27.2, and 115.4 Å in the three separate runs made with the system having an 80-monomer molecule (or 7.9, 17.6, 17.7, 22.4, 58.3, and 62.4 Å in the case of the system with two shorter molecules). Each of these numbers deviates substantially from 61.0 Å (or 43.0 Å), a value expected if the characteristic ratio $\langle r^2 \rangle / nl^2$ is equal to 10. The overall average of the end-to-end distances, however, comes to 69.6 Å (or 37.6 Å), much closer to the expected value. The radius of gyration is 13.3, 14.7, and 38.4 Å (or 10.6, 12.0, 12.2, 13.9, 18.3, and 19.9 Å), averaging to 25.0 Å (or 14.9 Å), in comparison to the expected value 22.3 Å (or 15.8 Å).[27] Despite these differences in the average chain dimensions, the X-ray diffraction curves obtained from the three runs differ from each other only to a minor extent (see part 1), suggesting that the subtle differences in the overall chain conformation do not appreciably modify the packing of neighboring segments that gives rise to the short range structure discussed in this work.

Distinction between *Intra-* and *Inter*molecular Pairs

We investigate the short range structure first by evaluating the radial distribution functions of the chain backbone segments and of the phenyl groups. For this purpose each of the phenyl groups is represented by a point located at its center and we evaluate the radial distribution of such center-of-mass points. In the case of chain backbones, a triplet of aliphatic carbon atoms C_{i-1}, C_i, and C_{i+1} is again represented by its center of mass. A curve connecting such a sequence (i = 2, ..., 79) of triplet centers-of-mass should coincide approximately with what one would regard as the (curved) axial core of the chain backbone. Before presenting the radial distribution functions of these center-of-mass points, we here make a little digression about the meaning of the words *intra-* and *inter*molecular.

In general with polymers, the distinction between *intra-* and *inter*molecular pairs is not clear cut. When a polymer molecule is extremely long (or in the case of a cross-linked network), essentially all the neighbor segments surrounding a given segment A belong to the same molecule. Yet most of these neighbor segments do not merit the term *intra*molecular, unless they are connected to segment A through only a short sequence of intervening covalent bonds. Any interaction between segment A and the rest of the neighboring segments is dominated by nonbonded forces and should be regarded as *inter*molecular in character. It is more appropriate to regard monomers i and j in the same molecule as an *intra*molecular pair only if the "monomer index difference" $m \equiv |i - j|$ is relatively small, and as *intermolecular* otherwise.

Another complication in separating *intra-* from *inter*molecular pairs arises in molecular modeling with

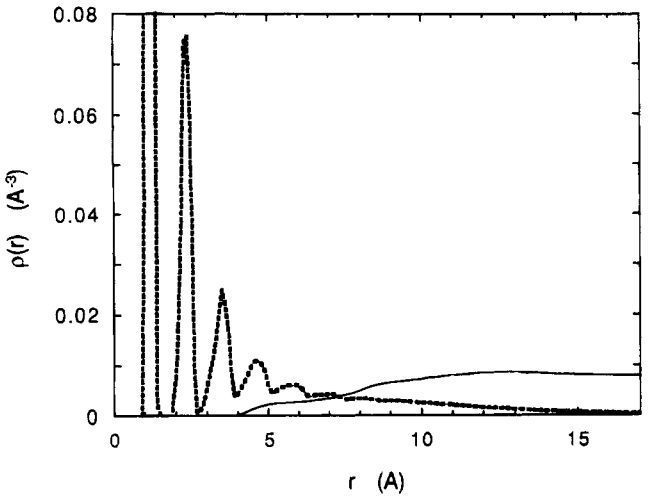

Figure 1. Radial distribution function $\varrho(r)$ of the center-of-mass of backbone carbon triplets. Here $\varrho(r)$ is the density of such triplet centers-of-mass that are found at distance r from a given triplet center-of-mass. The thin solid line gives the *inter*molecular pairs and the thick broken line the *intra*molecular pairs. These results were evaluated with the system containing a single polystyrene molecule of 80 monomers.

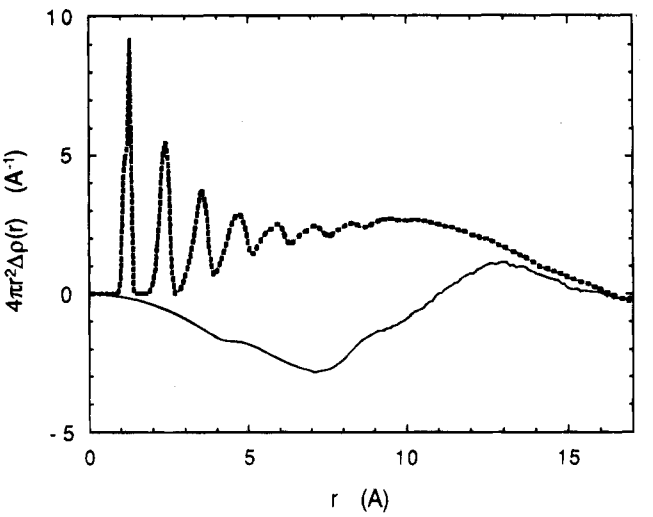

Figure 2. Data given in Figure 1 replotted so that the ordinate now gives $4\pi r^2[\varrho(r) - \langle\varrho\rangle]$, where $\langle\varrho\rangle$ is the average density of (either *intra-* or *inter*molecular) backbone carbon triplet centers-of-mass to be found around a given triplet center-of-mass. In such a "radial difference distribution function" plot the area under a peak is related to the actual number, rather than the density, of triplet centers found at distance r. Note that the curve giving the *inter*molecular correlation (thin solid line) starts out negative in the small r region, manifesting the so-called "correlation hole" effect.

periodic boundary conditions because of the presence of image molecules. If we consider the ith segment on molecule A and the jth segment on molecule B which is an image of A, there is obviously no sequence of covalent bonds that connects the two. However, when $m \equiv |i - j|$ is small, the status of the ith segment on molecule A influences the jth segment on the same molecule through bonded interactions, and hence influences the jth segment on molecule B indirectly.

To avoid any ambiguities that might arise from such complications, we have defined the *intra-* and *intermolecular* pairs in this work in the following manner, and differently for the two systems studied. With the system containing a single longer molecule, a pair of segments residing on the same molecule is regarded as *intra*molecular only when the monomer index difference m is equal to 10 or smaller. An *inter*molecular pair is one in which the second member resides on an image molecule and moreover the monomer index difference is larger than 10. This leaves some 20% of all possible pairs (the exact percentage depending on the distance range included in the analysis) in the unclassified category which belongs to neither *intra-* nor *inter*molecular. With the system containing two shorter molecules, a different strategy is adopted. Here all pairs of segments residing on the same molecule are considered *intra*molecular, while a correlation between a segment on molecule A with a segment on a different molecule B or an image of B is considered *inter*molecular. In this case some 40% of the pair correlations are left out in the indeterminate category.

Figure 1 shows the radial distribution function $\varrho(r)$ of the backbone atom triplet centers-of-mass, evaluated for the system with a single 80-monomer molecule. Here $\varrho(r)$ represents the density (in Å^{-3}) of triplet centers found at distance r from a given triplet center. The thick dotted line is for the *intra*molecular pairs and the thin solid line for the *inter*molecular pairs, the distinction between them made according to the definition given above. As r increases, the *inter*molecular radial distribution function approaches the average density $\langle\varrho\rangle$, whereas the *intra*molecular function gradually diminishes toward zero. At small r, much fine structure is seen in the *intra*molecular function, but the *inter*molecular function is practically zero for r below about 4 Å.

The same data in Figure 1 are replotted in Figure 2 where the ordinate is now $4\pi r^2[\varrho(r) - \langle\varrho\rangle]$. A plot of $4\pi r^2\Delta\varrho$, which is referred to as the "radial difference distribution function" (RDDF), is often more informative than a plot of $\varrho(r)$ itself, since now the area under a peak represents the actual number, rather than the density, of triplet centers found at distance r. [When $\varrho(r)$ stands, for example, for the density $\varrho_{\text{intra}}(r)$ of *intra*molecular triplet centers surrounding a given center, $\langle\varrho\rangle$ now stands for the average of $\varrho_{\text{intra}}(r)$ throughout the system.] We note that the *inter*molecular $4\pi r^2\Delta\varrho(r)$ function is negative initially when r is relatively small, until r exceeds about 11 Å. This is a manifestation of the "correlation hole" effect, first pointed out by deGennes, that arises from the fact that atoms belonging to other molecules tend to be excluded from the vicinity of a given molecule. Figure 3 plots the similar results evaluated with the system containing two smaller molecules. Here the negative region for the *inter*molecular correlation extends to only about 9 Å, reflecting the fact that the molecules are now smaller. Other than that, the overall features in Figures 2 and 3 are very similar to each other, especially for r relatively small, despite the distinct difference between the two systems in the way the *intra-* and *inter*molecular division is defined.

In Figure 4 we present the RDDF of the centers of mass of phenyl groups evaluated for the longer molecule system. The *intra*molecular RDDF shows, as expected, some fine structures. The *inter*molecular function is strongly negative throughout the r region shown, again manifesting the correlation hole effect. It is surprising to see, however, a sharp, prominent peak centered at 6.0 Å. This 6 Å peak is the most conspicuous feature that characterizes the *inter*molecular phenyl–phenyl correlations in polystyrene. Figure 5 shows the phenyl mass-center RDDF evaluated for the shorter molecule system. The *inter*molecular peak centered around 6 Å is as prominent as in Figure 4. In view of the close

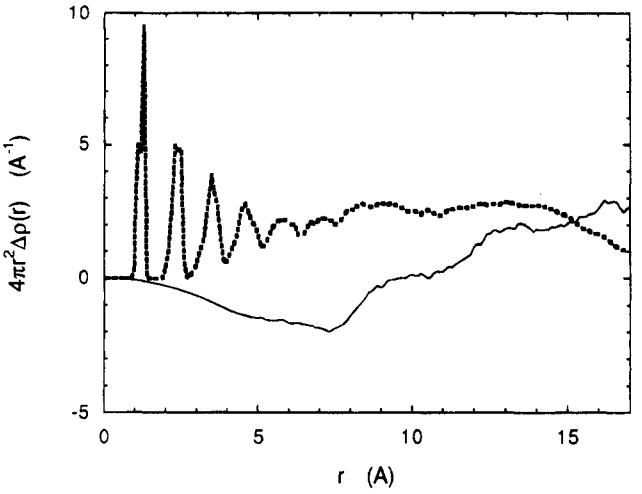

Figure 3. Plotted data similar to those given in Figure 2, but now showing results obtained with the system containing two polystyrene molecules of 40 monomers each. The slightly different criteria used here in differentiating the *intra-* from *inter*molecular pairs led to the changes in the plots at large r from Figure 2, but the overall qualitative features remain the same. The reduced negative region in the *inter*molecular correlation (thin solid line) reflects the reduced range of the "correlation hole" effect around a shorter molecule.

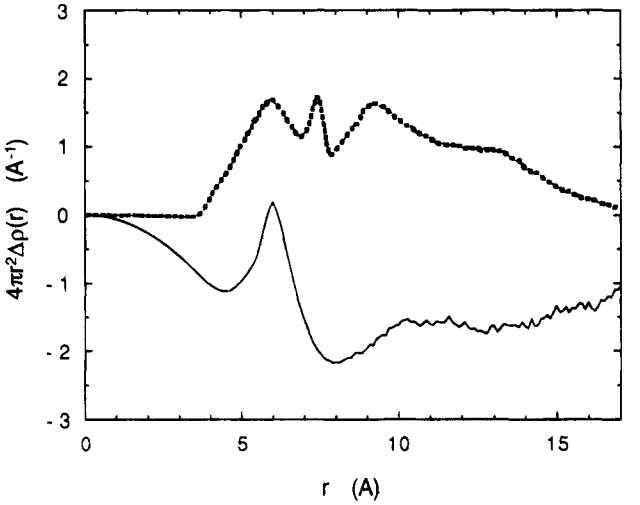

Figure 4. Radial difference distribution functions of phenyl centers-of-mass. The thick broken line gives the *intra*molecular correlation, and the thin solid line, the *inter*molecular correlation. These data were obtained with the system containing a single 80-monomer molecule. The most prominent feature is the presence of a strong *inter*molecular correlation around a 6 Å distance.

similarities exhibited by these two systems, from now on we examine only the longer molecule system as we probe the further details of the *intra-* and *inter*molecular correlations as described below.

*Intra*molecular Correlations

In Figure 6 we plot the functions $4\pi r^2\Delta\varrho(r)$ of *intra*molecular phenyl center pairs evaluated individually according to the monomer index difference m. Phenyl pairs which are first neighbors along the chain ($m = 1$) are naturally confined to a close vicinity of each other in space (r less than 8 Å). The range of distances available to neighbors gradually extends to larger r as the monomeric distance m along the chain is increased. The overall appearance of the curves in Figure 6 suggests that the r range centered around 6 Å and extending from about 4 to 8 Å might be recognized,

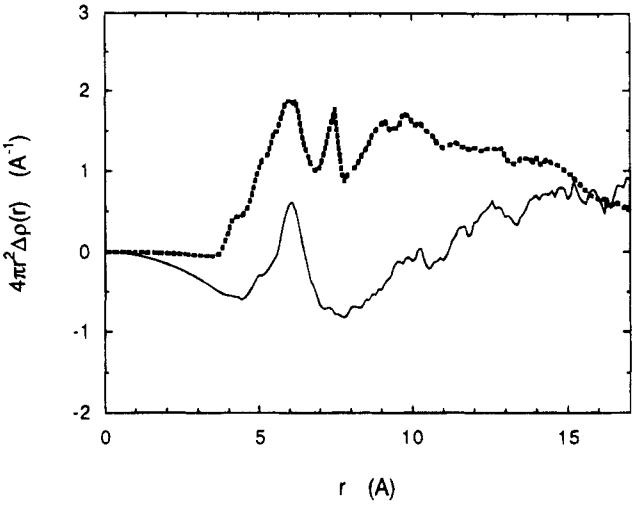

Figure 5. Data similar to those in Figure 4 but evaluated with the system containing two 40-monomer molecules. Although details are different (the difference resulting partly from the different criteria for differentiaing *intra-* and *inter*molecular pairs), the overall qualitative features are seen to remain unchanged.

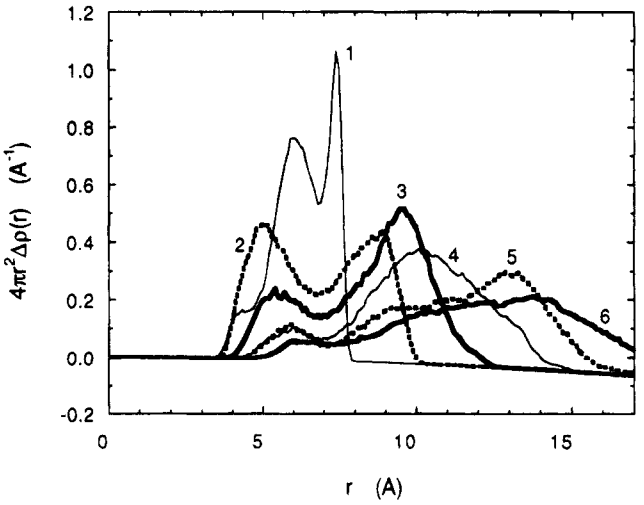

Figure 6. *Intra*molecular correlation of phenyl centers-of-mass now evaluated individually according to the "monomer index difference" $m = |i - j|$ indicated for each curve. Note that many of the second monomeric neighbors approach each other closer than some of the first monomeric neighbors do.

somewhat arbitrarily, as the first coordination shell for *intra*molecular phenyl–phenyl pairing. It is then seen that the contribution of phenyls to this first coordination shell steadily decreases, as one would expect, as the monomer index difference m increases.

The first neighbor phenyls ($m = 1$), although they all belong to the first coordination shell defined above, divide themselves into three groups according to the shape of the RDDF curve seen in Figure 6. The first group is represented by the small peak (or shoulder) centered around 4.3 Å, the second by the large peak centered around 6.0 Å, and the third by the narrow peak around 7.3 Å. Evaluated from the areas under the peaks the numbers of phenyls belonging to the first group (3.5–4.8 Å), the second (4.8–6.9 Å), and the third (6.9–8.0 Å) are 0.17, 1.20, and 0.61, respectively.

The second monomeric-neighbor pairs ($m = 2$) divide themselves fairly cleanly into two groups, one centered around 5.0 Å and the other around 8.8 Å. If we take the boundary between these two to be at 6.8 Å, exactly half of them belong to the first group and the rest to

the second. In comparing the RDDF curves for $m = 1$ and $m = 2$, we note that a good fraction of the second neighbor pairs have a separation distance smaller than the majority of the first neighbor pairs have. This has an interesting implication touching upon a basic assumption underlying the rotational isomeric states model method. The RIS model assumes[28,29] that the conformation of a vinyl-type polymer chain can be adequately described by consideration of interactions between atoms separated at most by four covalent bonds (i.e., up to the "second-order interactions" only). It is this assumption that allows the statistical weight matrix to be evaluated from a calculation of the conformation energy map of chain backbone diads only. However, the above finding that second neighbor phenyls approach more closely to each other than first neighbor phenyls do suggests that the interaction between second neighbor phenyls may have a much stronger influence than previously assumed on the relative stability of various diad conformations. In other words, neglecting the effect of the so-called "third and higher order interactions", as has been customary in the RIS calculations of vinyl polymers, may not be warranted, and instead the conformational energy maps involving torsional rotation angles of three or more successive backbone bonds may have to be examined in the case of polystyrene (and possibly for some other vinyl polymers).

To see the geometric relationship between the two phenyls approaching each other, we need information not only on the distance r between their centers but also on their mutual orientation. As an aid in this effort, we associate with each phenyl group two vectors defining its orientation: $\mathbf{z}$ the vector normal to the phenyl plane, and $\mathbf{x}$ the vector pointing from the phenyl center to the *para* carbon. We then characterize the orientation of phenyl i with respect to phenyl j by means of the four angles θ_z, θ_x, ψ_z, and ψ_x defined as follows. θ_z is the angle between $\mathbf{z}_i$ and $\mathbf{z}_j$, θ_x is the angle between $\mathbf{x}_i$ and $\mathbf{x}_j$, ψ_z is the angle between $\mathbf{z}_i$ and the vector $\mathbf{R}_{ij}$ linking the center-of-mass of phenyl group i to that of phenyl group j, and ψ_x is the angle between $\mathbf{x}_i$ and $\mathbf{R}_{ij}$. (Note that θ_x and ψ_x vary from 0 to π, while θ_z and ψ_z vary from 0 to $\pi/2$ because of the mirror symmetry about the phenyl plane.) From the atomic coordinates obtained in the simulation we then evaluate the order parameter $S(\alpha)$ for angle α as a function of r, where $S(\alpha)$ is the average of the second Legendre function $P_2(\cos\alpha) = (3/2)(\cos^2\alpha) - 1/2$.

To aid the visualization and description of the geometry of approach of two phenyls, some simple examples are sketched in Figure 7. The separation vector $\mathbf{R}_{ij}$ is indicated by the broken line. The corresponding values of the angles θ_z ,ψ_z, θ_x, and ψ_x are listed in Table 1. (In the case of geometry C, the values of ψ_z and ψ_x for the two members of the pair are different from each other, and the first one given is for the phenyl on the left and the second one for the phenyl on the right.) Some other geometries can be thought of as derivatives of one of these prototype forms. For example, there could be many other "edge-to-edge" geometries with the "twist" angle (θ_z in this case) intermediate between 0 and 90°. Or, we might have a modified "face-to-face" geometry in which the "twist" angle (θ_x in this case) is not equal to 180° as in D. A geometry intermediate between A and C might involve a rotation of the right phenyl in A by an angle α about an axis perpendicular to the plane of the diagram. In this case the angles θ_z, ψ_z, θ_x, and ψ_x will have changed to α, 90° − α, 180° − α, and α, respectively.

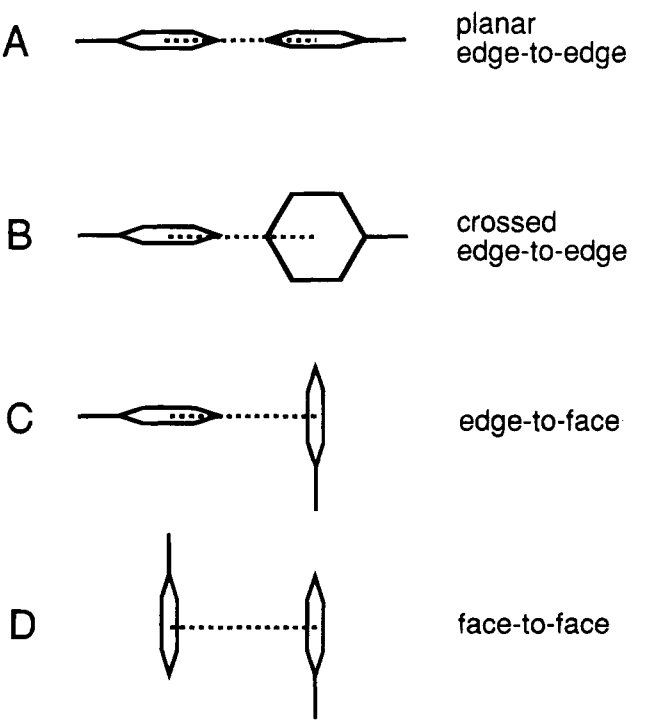

Figure 7. Some simple examples of the geometrical arrangement of two phenyl groups. The dotted line is the vector $\mathbf{R}_{ij}$ connecting the centers of the two phenyl groups.

Table 1. Angles Describing the Mutual Orientation of a Phenyl Group Pair in the Geometries Shown in Figure 7

	geometry	θ_z, deg	ψ_z, deg	θ_x, deg	ψ_x, deg
A	(planar edge-to-edge)	0	90	180	0
B	(crossed edge-to-edge)	90	90	180	0
C	(edge-to-face)	90	90	90	0
			0		90
D	(face-to-face)	0	0	180	90

Figure 8 plots the order parameters $S(\theta_z)$, $S(\psi_z)$, $S(\theta_x)$, and $S(\psi_x)$ that describe the relative orientation of first neighbor phenyl pairs ($m = 1$). As remarked earlier, the RDDF curve shows that the first neighbor phenyl pairs divide themselves into three groups. For those with separation distances r around 4 Å or less, the four parameters are all consistent (cf. Table 1) with geometry D ("face-to-face") in Figure 7. Obviously, only a parallel stacking is sterically allowed when two phenyls are to approach so close to each other, but of course the probability of such a close approach is also very small (about 9%). Some 30% of the pairs are at separation distances around 7.3 Å, and for these both $S(\theta_x)$ and $S(\psi_x)$ are not very far below unity, indicating that they are probably in the "edge-to-edge" geometry (see Table 1). The relatively small values of $S(\theta_z)$ and $S(\psi_z)$ suggest, however, that the "twist" angle is not confined to any fixed value, but rather distributed over a range of different values. For the majority of the pairs (with r around 6 Å), the four parameter values are all relatively small, and this probably signifies that the mutual orientations are fairly random and no single unique geometry can be assigned to this group.

Plots similar to those shown in Figure 8, but evaluated for $m = 2$ and $m = 3$, are given in Figures 9 and 10. For $m = 2$, the pairs at r around 5 Å or less appear to maintain the "face-to-face" geometry to a great extent, but the degree of parallelism seems to deteriorate very rapidly as r increases beyond 5 Å. For the second and

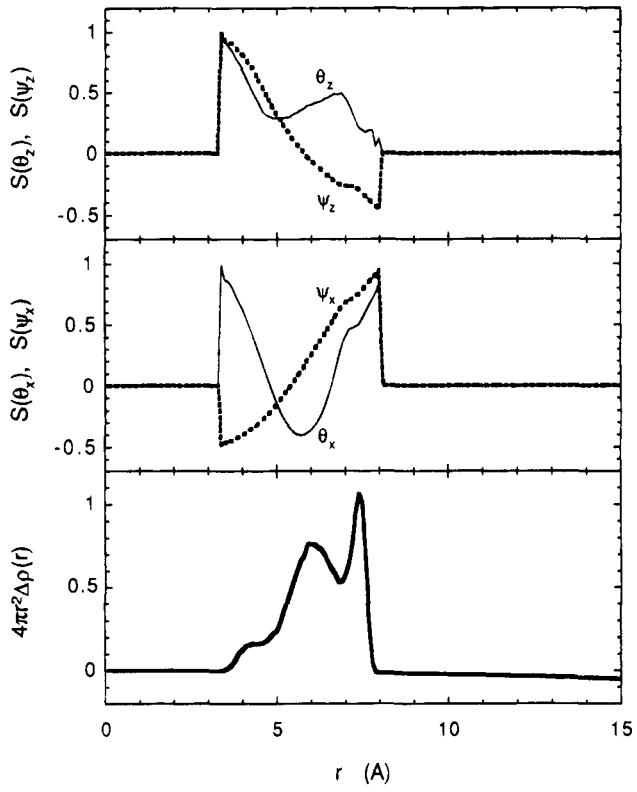

Figure 8. Order parameters (or the averaged second Legendre functions of the cosine) of θ_z, ψ_z, θ_x, and ψ_x plotted to see the mutual orientation of *intra*molecular first neighbor (m = 1) phenyl pairs. Here z is the axis perpendicular to the phenyl plane, and x is the axis directing from the center to the *para* carbon atom. θ is the angle between the similar axes in the two phenyls, and ψ is the angle which such an axis makes with the center-to-center vector $\mathbf{R}_{ij}$. The values of the order parameters are statistically meaningful only when a sufficient number of pairs are available at the given distance r, as indicated by the radial difference distribution function shown.

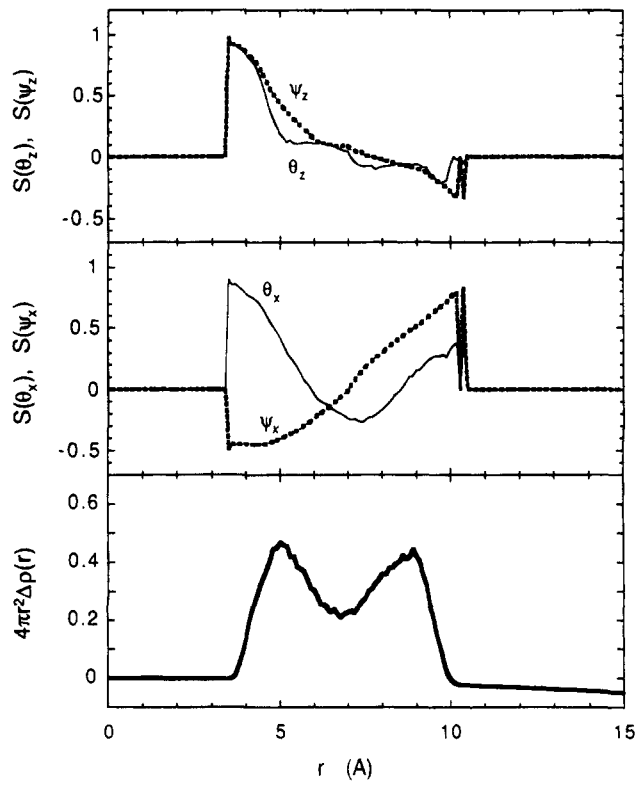

Figure 9. Similar to Figure 8, but evaluated for *intra*molecular second neighbor phenyl pairs (m = 2).

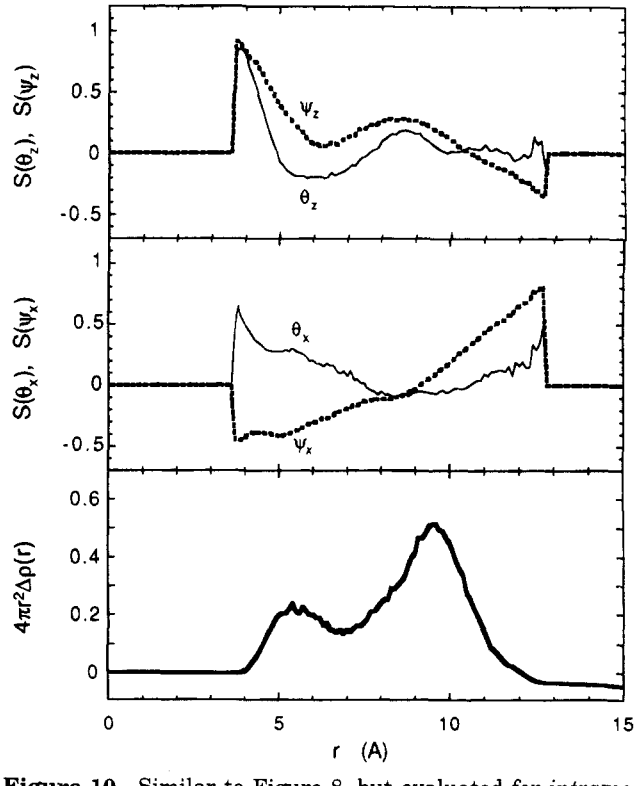

Figure 10. Similar to Figure 8, but evaluated for *intra*molecular third neighbor phenyl pairs (m = 3).

third neighbor pairs at r larger than 6 Å, no single geometry appears to dominate and a continuous range of many different types of geometries are probably involved.

The more customary way of examining the *intra*molecular structure is to evaluate the torsional rotation angles of a pair of succeeding bonds (i, i + 1) along the chain backbone. Figure 11 gives the contour map for population distribution of a meso diad evaluated as a function of (ϕ_i, ϕ_{i+1}), and Figure 12 gives a similar plot for a racemic diad. Here ϕ is defined to be 0 for the trans conformation, and the positive and negative directions of the ϕ angle are taken in the sense described by Flory et al.[29] The contour lines drawn correspond to R = 1, 2, 4, 8, 16, and 32, where the R value signifies that the population found at the given ϕ_i and ϕ_{i+1} is equal to R times the population that would have been realized if the distribution were random. Since the population distribution should be proportional to exp($-E/kT$), the contour lines in Figures 11 and 12 should correspond to contour lines in a conformational energy map drawn at equal energy increments. Such a potential energy map was calculated by Yoon, Sundararajan, and Flory[30] as a precursor to the application of the RIS model method to conformational properties of polystyrene. A similar calculation was performed again recently by Rabold and Suter.[31] In these calculations interactions between atoms separated by more than four intervening covalent bonds (the so-called third and higher order effects), as well as *inter*molecular interactions, were neglected. The force field parameters employed in these works were also different from ours. Yet we see a great deal of similarity between the energy maps produced by these two groups of workers and the population distribution maps given in Figures 11 and 12. For example, for meso diads the highest populations

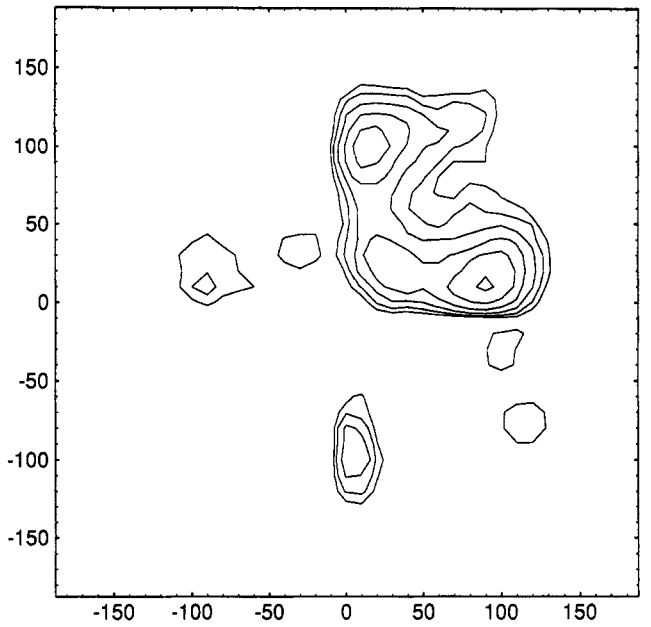

Figure 11. Contour map showing the population distribution of backbone bond torsion angles (ϕ_i, ϕ_{i+1}) in meso diads. ϕ = 0 corresponds to the trans state, and the positive direction of ϕ is defined as described by Flory et al.[29] The contour lines are drawn at $R(\phi_i,\phi_{i+1})$ equal to 1, 2, 4, 8, 16, and 32, where the R value signifies that the population found at the given ϕ_i and ϕ_{i+1} is equal to R times the population that would have been available if the distribution were random.

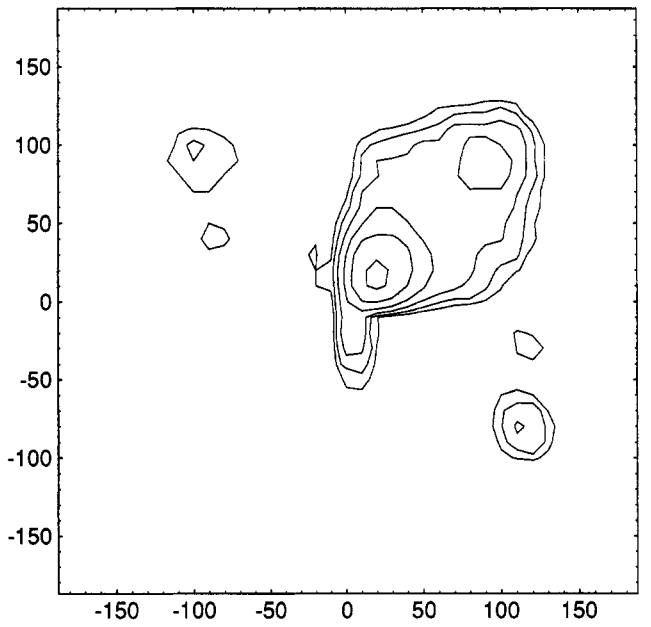

Figure 12. Similar to Figure 11, but evaluated for racemic diads.

are at tg and gt conformational states and for racemic diads they are at tt and gg states. There are also discrepancies of ours from these previous results, and among them we note the following three points. First, in the population distributions obtained in this work, the most probable torsional angle for the gauche state has been reduced to about 90° from its intrinsic 120° angle, and at the same time the most probable torsional angle for trans state has increased to about 20°, thus bringing the trans and gauche states much closer together. Second, in the racemic diad the importance of tg and gt states has been much reduced in comparison to the energy maps produced by YSF and RS. Third,

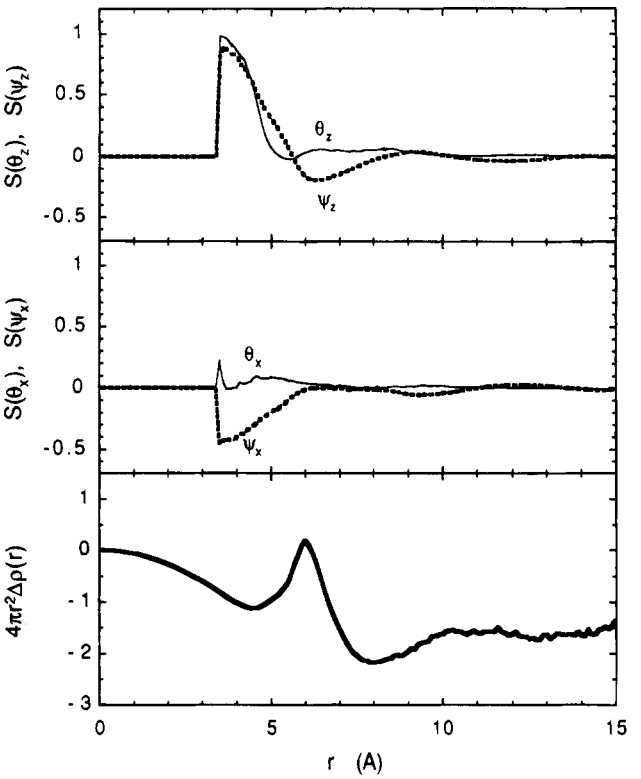

Figure 13. Similar to Figure 8, but evaluated for *inter*molecular phenyl pairs.

the main difference between the results by YSF and RS is in the relative importance of tt and gg states in the meso diad, and our results show that tt states are more highly populated than gg states, more in agreement with the YSF energy map.

The differences between our population map and the YSF and RS energy maps could have arisen from three possible sources: (a) the differences in the force field parameters used, (b) the influence of the third and higher order *intra*molecular effect on the chain conformation, and (c) the effect of *inter*molecular interactions exerted by neighboring molecules in the bulk polymer. The second aspect is important if we are to understand the degree of accuracy in the single chain conformational properties that one can expect from the customary RIS method neglecting the higher order effects. The third aspect is important if we are to understand the accuracy to which the conformational properties of molecules in the bulk polymer can be represented by the single chain properties evaluated either by the RIS or by any other experimental or computational method. The fact that the end-to-end distance and other average parameters specifying the overall chain conformation in the bulk state agree with those in the theta solution may not necessarily imply that the local structure in the distance scale of interest here is not affected by the presence of neighboring molecules. Clarification of these points would require a set of related studies in which the same force field parameters are applied consistently.

*Inter*molecular Correlations

Figure 13 plots the values of the order parameters $S(\theta_z)$, $S(\psi_z)$, $S(\theta_x)$, and $S(\psi_x)$ evaluated for the *inter*molecular phenyl pairs. For the very small population found at distances below about 4.5 Å the data $S(\theta_z)$ = $S(\psi_z)$ = ~1 and $S(\psi_x)$ = ~−0.5 are consistent with the "face-to-face" geometry D given in Figure 7, except that

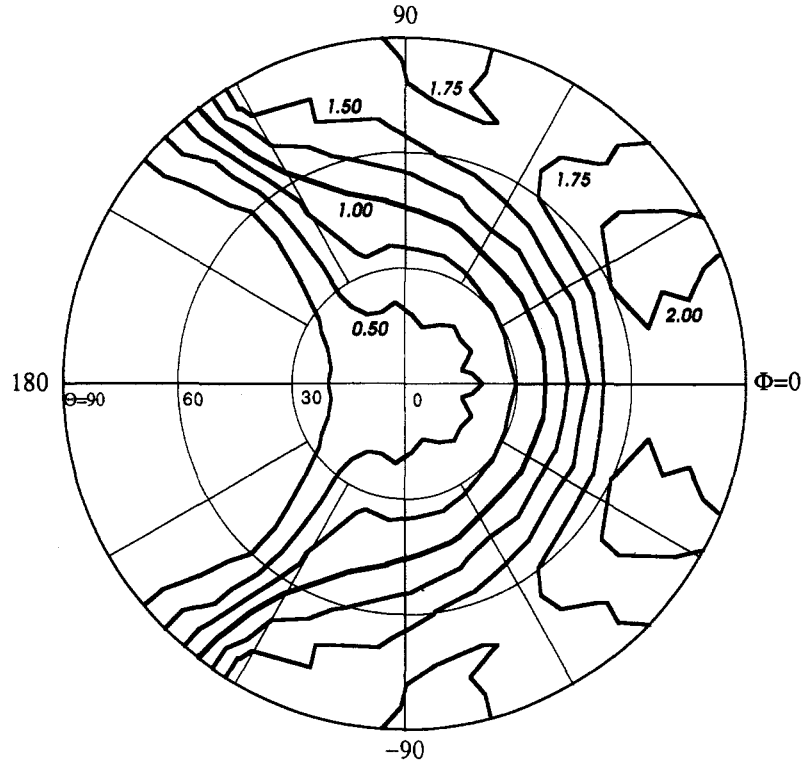

Figure 14. Plot showing the probability, given a phenyl group at the origin, that a second *inter*molecular phenyl group is to be found at a distance 5.5 Å < r < 6.5 Å in direction (Θ,Φ). Let a phenyl group be at the origin of a coordinate system O-*XYZ*, lying horizontally and with its *para* carbon atom pointing along the X axis (Φ = 0). The Θ = 0 direction is along the (vertical) Z axis perpendicular to the phenyl plane. Now imagine two spherical surfaces of radius 5.5 and 6.5 Å, respectively, surrounding the origin. Next evaluate the population of *inter*molecular phenyls found between the two spherical surfaces in the direction specified by Θ and Φ. The contour lines give the $R(\Theta,\Phi)$ values which are proportional to the populations thus found. $R(\Theta,\Phi)$ = 1 means that the population is the same as would be found if the distribution of the second phenyls were random in all directions. The contour map shows, for example, that the population in the region $|\Phi| > 135°$ is very low, where the access is blocked by the presence of the chain backbone to which the first phenyl is attached.

$S(\theta_x)$ = ~0 indicates that the "twist" angle (i.e. the angle of rotation around the common z axis) is distributed random. At distances larger than 8 Å all the four order parameters are almost equal to zero, indicating that essentially no orientational correlations exist at these separation distances.

As remarked in connection with Figures 4 and 5, the most striking feature in the *inter*molecular phenyl–phenyl correlation is the high frequency of occurrence of 6 Å separation. We now set out to examine the mutual orientation of the two phenyls at this separation in more detail than can be gauged from the four order parameters. For this purpose, we set up a coordinate system O–*XYZ* fixed with the first member of the phenyl pair and ask in which direction the second member is located when it is at a distance between 5.5 and 6.5 Å. The origin O of the coordinate system is placed at the center of the first phenyl, and Z and X axes coincide with its z and x axes, respectively. We then evaluate the probability of finding another phenyl at a distance r between 5.5 and 6.5 Å as a function of Θ and Φ, the customary polar coordinate angles. The result is presented in Figure 14 as a contour plot of quantity $R(\Theta,\Phi)$. Here $R(\Theta,\Phi)$ is the population $P(\Theta,\Phi)$ of the second phenyl found in the direction (Θ,Φ) divided by the population $P_{\text{random}}(\Theta,\Phi)$ that would have been found if the distribution were random. In other words, contour levels higher than unity correspond to a more frequent occurrence than in a random distribution. We see that in the general direction $|\Phi| > 135°$ $R(\Theta,\Phi)$ is very small, in agreement with the obvious expectation that the chain backbone attached to the phenyl prevents other phenyls from approaching. In general $R(\Theta,\Phi)$ values increase as Θ increases toward 90°. This shows that the center of the second phenyl tends to be in the vicinity of the equatorial region defined by the extension of the first phenyl plane. The highest $R(\Theta,\Phi)$ values are found at Θ = ~75° and Φ = ~±25°, and second maxima exist at Θ = 90° and Φ = ±85°. On the equatorial plane (θ = 90°), the Φ values of ±30° denote the directions that bisect the *para* and *meta* carbon atoms and those of ±90° the directions that bisect the *meta* and *ortho* carbon atoms, both directions in which the steric interference due to the presence of hydrogens attached to the carbons is expected to be the least. (It is interesting to note that even in the absence of explicit hydrogens in the united atom model, the geometry of steric interferences is well represented.)

Now that we have determined the positions of the second phenyl centers with respect to the first, we next examine the orientations of these second phenyls. Some inference can be made on the orientation of the second phenyl from a symmetry consideration alone. For example, since the second phenyl center tends to be around the equatorial region of the first phenyl, by symmetry the second phenyl should be oriented in general to have its edge pointing toward the first phenyl center. To probe further, we focus on a selected group of second phenyls that are in the direction of higher probabilities, that is, those which are located in the direction $\Theta > 56°$ and $|\Phi| < 90°$. These directions correspond roughly to the regions bound by the contour lines of $R(\Theta,\Phi)$ = 1.75 in Figure 14. About 51% of all the *inter*molecular phenyl pairs in the distance r

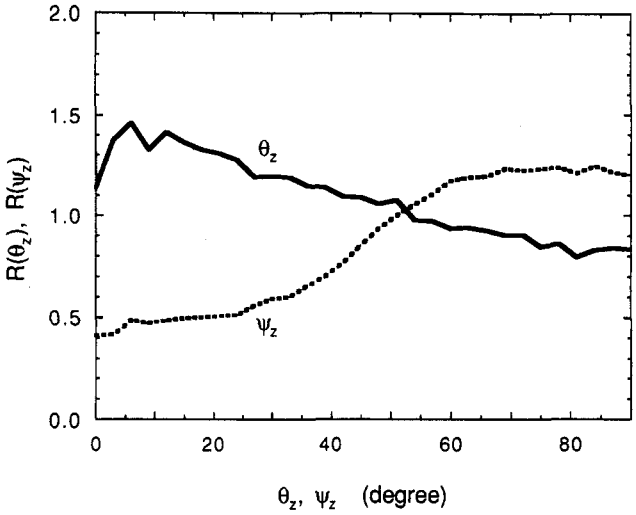

Figure 15. Distributions of θ_z and ψ_z angles, where θ_z is the angle between the z axes of two phenyls and ψ_z is the angle between the center-to-center vector **R** and the z axis of the second phenyl. The value of $R(\theta_z)$ is equal to the population $P(\theta_z)$ of second phenyls having the particular θ_z divided by $P_{\text{random}}(\theta_z)$ that would have been realized if the distribution were random. $R(\psi_z)$ is defined similarly. The distributions shown here were evaluated for the selected group of second phenyls located in the direction $\Theta > 56°$ and $\Phi < 90°$ and at the distance r between 5.5 and 6.5 Å from an arbitrarily chosen first phenyl.

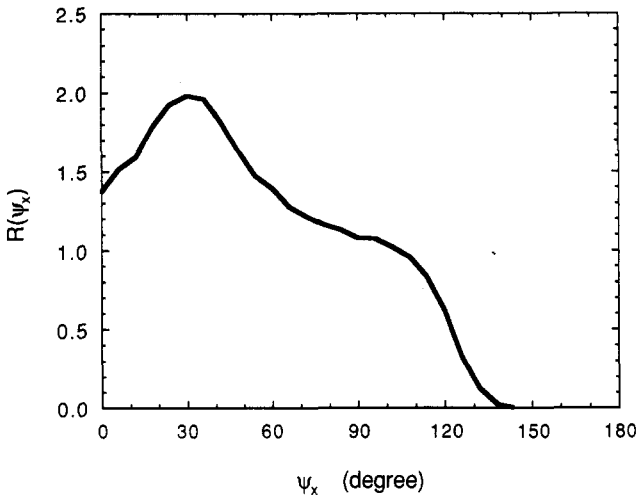

Figure 16. Similar to the distributions shown in Figure 15, but with $R(\psi_x)$ where ψ_x is the angle between the x axis of the second phenyl and the center-to-center vector **R**.

between 5.5 and 6.5 Å belong to this group. The distributions of the angles θ_z, ψ_z, and ψ_x evaluated for this selected group of phenyls are presented in Figures 15 and 16. The quantities plotted are the relative frequency distribution $R(\alpha)$, denoting the number $P(\alpha)$ of phenyls characterized by a value of the angle α in the selected population divided by the similar number $P_{\text{random}}(\alpha)$ that would have been realized if the distribution were random. ψ_z is the angle between the vector **R**, pointing from the center of the second phenyl to that of the first, and the z axis (normal to the phenyl plane) of the second phenyl. Figure 15 shows that $R(\psi_z)$ is larger for larger ψ_z angles. This means that the geometry of phenyl pair arrangement is essentially based on the edge-to-edge arrangements shown as geometries A and B in Figure 7. The information on the "twist" angle between the two phenyl planes can be obtained by looking at the distribution $R(\theta_z)$, where θ_z is the angle between the z axis of the first phenyl (Z axis) and the z axis of the second phenyl. $R(\theta_z)$ is greater than unity for smaller θ_z values, and this means that the planar edge-to-edge (geometry A) is more favored than the crossed edge-to-edge (geometry B), but all the intermediate values of the "twist" angles are also available. Finally, Figure 16 shows the values of $R(\psi_x)$, where ψ_x is the angle between the x axis (or *para* axis) of the second phenyl and the center-to-center vector **R**. There is a maximum around $\psi_x = 30°$ and an indication of a weak maximum around $\psi_x = 90°$, both of which are consistent with the maxima in the $R(\Theta,\Phi)$ plot in Figure 14 near $|\Phi| = 25$ and 85° in the equatorial region.

Thus we come to the conclusion that the most probable configuration of the approach of two *inter*molecular phenyls to a distance of 6 Å resembles the edge-to-edge geometries given in Figure 7, but with some modifications. To visualize such configurations, we start with a pair of phenyls 6 Å apart in the planar edge-to-edge arrangement. One or both phenyls are then rotated around their own z axes to as to bring the phenyl hydrogens in the staggered positions minimizing steric interferences. The right phenyl is now rotated around the center-to-center axis to a "twist" angle anywhere between 0° (planar edge-to-edge) and 90° (crossed edge-to-edge), but with a higher probability for a smaller value. Finally, the axis between the two centers is bent in the middle by about 25° so as to bring the right phenyl center above the plane of the left phenyl. The above pictorial description is meant to be only an approximate, heuristic one, and whenever such a presentation is made, one has to hasten to qualify it by saying that there exists in reality a broad distribution of geometries with the various angles defining them varying continuously over broad ranges. When we made graphic displays of a large number of phenyl pairs on a computer screen, it was difficult to recognize any specific geometric patterns, and the arrangements appeared to be more-or-less random. The above "most probable geometry" should therefore be regarded not as a faithful representation of a few "typical" pairs, but rather as a composite picture emerging from a statistical average of a large number of such pairs.

As another means of gauging the short range order, we evaluate the coordination number of phenyls, that is, the number of nearest neighbor phenyl groups surrounding a given phenyl group. The shape of the *inter*molecular RDDF in Figure 4 suggests, with little ambiguity, that the first coordination shell can be taken to extend up to about 8 Å around a phenyl group. This is also consistent with the 8 Å coordination shell for *intra*molecular phenyl pairs, assigned earlier in discussing the features in Figure 6. From an integration of the area under the peak in the RDDF in Figure 4, we find that the coordination shell of radius 8 Å contains 12.3 phenyl neighbors surrounding a given phenyl group. Of these, 1.1, 7.7, and 3.9 phenyls are in the distance ranges 4–5, 5–7, and 7–8 Å, respectively, or in terms of densities, 4.32, 8.45, and 5.57 phenyls/1000 Å^3 in the respective distance ranges. Of the total 12.3 phenyls in the coordination shell, about 5.1 are *intra*molecular with $m \leq 10$, about 5.5 are *inter*molecular (in the sense of the word as discussed in conjunction with Figures 2 and 4), and 1.7 are in the unclassified category. Incidentally, a graphical examination of the contents of the coordination shell failed to give any evidence suggesting a preference by the phenyls to

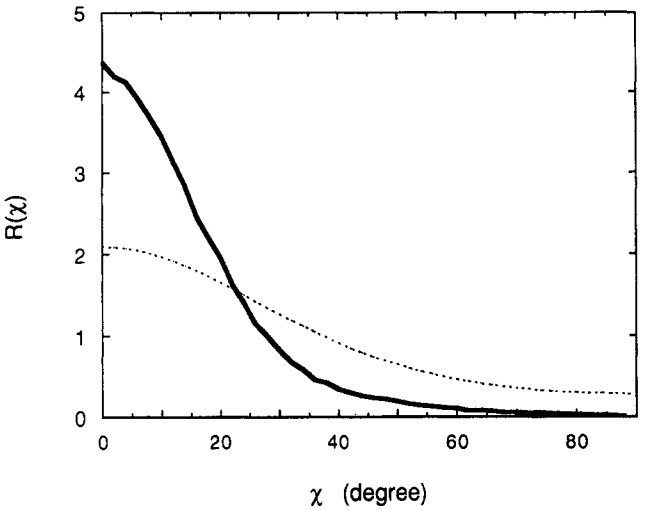

Figure 17. Population distribution of χ angles, where χ denotes the torsion angle of the bond that connects a phenyl to the aliphatic methine carbon. Here χ is defined to be 0° when the phenyl plane is perpendicular to the backbone direction. $R(\chi)$ is the relative population at an angle χ in comparison to a random distribution. The dotted line gives the Boltzmann distribution which would have been realized if there were no hindrances to the torsional rotation except for the 2 kcal/mol ad hoc barrier imposed in the model.

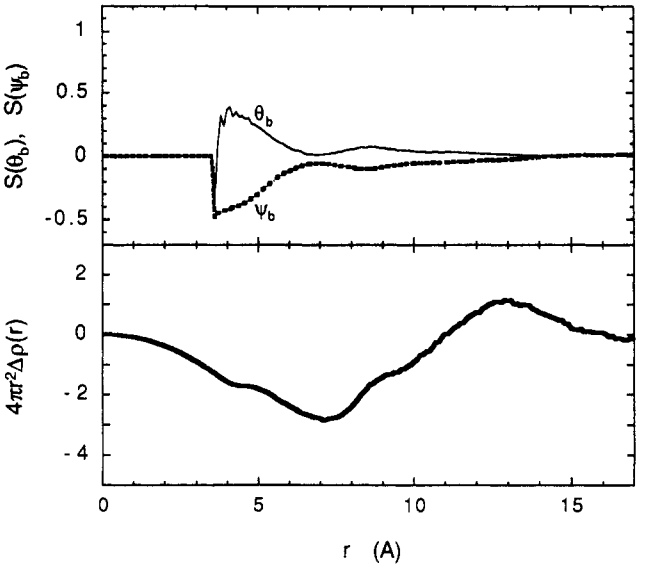

Figure 18. Backbone direction represented by vector $\mathbf{b}_i$ which connects the midpoint of the $C_{i-1}-C_i$ bond to the midpoint of the C_i-C_{i+1} bond. Plotted here are the order parameters of angles θ_b and ψ_b giving the mutual orientation of an *inter*molecular pair of such vectors as a function of the separation distance r between them. Note that the order parameters are nearly equal to zero for all r greater than about 6 Å, showing that there is very little tendency for the backbones to pack parallel.

cluster in triplets or quadruplets either *intra-* or *inter*molecularly.

Finally, we examine the orientation of *inter*molecular pairs of aliphatic backbones. Before going into the analysis of backbone orientations, we first note that the backbone direction at any point along the chain coincides approximately with the z axis of the phenyl which is appended to it. This is because the torsion angle χ of the bond joining the methine carbon to the phenyl ring is usually narrowly confined to around zero, as has been noted by several groups of workers in the past.[30,32,33] Figure 17 gives the distribution of χ evaluated from our MD results. Here we digress a little. Such a χ angle range restriction is considered to arise from steric hindrances between the ortho hydrogens in the phenyl and the aliphatic hydrogens. In the absence of these hydrogens in our united atom model, we imposed an ad hoc χ torsion barrier of 2 kcal/mol to take the place of such steric hindrances. If there were present no other hindrances to the torsional rotation, the χ angle distribution would have been given by the Boltzmann distribution, shown in Figure 17 by a thin broken line (calculated for $T = 500$ K). The actual χ angle distribution realized in our MD runs turns out to be much narrower than this Boltzmann distribution, suggesting that the nonbonded interactions between united carbon atoms by themselves are sufficient to produce the required barrier to χ torsion, and the ad hoc torsional potential would not have been necessary.

To specify the direction of the chain backbone, we define vector $\mathbf{b}_i$ connecting the midpoint of the $C_{i-1}-C_i$ bond to the midpoint of the C_i-C_{i+1} bond. The mutual orientation of two such vectors $\mathbf{b}_i$ and $\mathbf{b}_j$ separated by a distance r is then studied by examining the two angles, θ_b and ψ_b, defined in a similar manner as before; that is, θ_b is the angle between the two vectors $\mathbf{b}_i$ and $\mathbf{b}_j$, and ψ_b is the angle which $\mathbf{b}_i$ makes with vector $\mathbf{R}_{ij}$ of length r connecting the center-of-mass of triplet i to that of triplet j. The order parameters $S(\theta_b)$ and $S(\psi_b)$ are then evaluated for *inter*molecular pairs of backbone carbon triplets and are plotted in Figure 18. When r is smaller than about 5 Å, $S(\theta_b)$ is positive while $S(\psi_b)$ is negative, indicating that the chain backbones tend to be parallel to each other. The population of backbone pairs that come to such short distances is of course fairly small. For all distances above around 6 Å, the order parameters are nearly equal to zero, indicating that there is very little tendency for the chain backbones to line up parallel. In addition to looking at the averaged Legendre functions, we have also evaluated the distributions (not shown here) of the θ_b and ψ_b angles for those pairs with r between 11 and 15 Å. The distributions turn out to be almost completely flat, thus confirming the almost total lack of correlations in the orientation of *inter*molecular backbone pairs. The slightly loose coupling of the phenyls to the backbone, revealed by a 20° spread in the χ angle distribution seen in Figure 17, is therefore sufficient to prevent the orientational order present in the packing of phenyls from propagating to the attached backbones.

Discussion

Narten determined the X-ray diffraction pattern of liquid benzene[34] and, by comparing it with a model based on the RISM theory,[35] concluded[36] that the first neighbor shell extending to 8 Å around a benzene center contained 12 neighboring molecules, with the maximum probability being around 6 Å. This is very similar to what we have concluded from the analysis of the data in Figure 4, as discussed earlier. In crystalline benzene[37] a molecule has twelve nearest neighbors, four each at the distance of 5.12, 5.97, and 6.10 Å. Burley and Petsko[38] made a survey of crystal structures of peptides and proteins having aromatic side chains and found that the histogram of the distances between the centers of mass of these side groups peaked sharply at about 5.8 Å. Thus the preponderance of 6 Å separation between phenyl centers appears to be a characteristic common to most substances having phenyl side groups, both crystalline and amorphous, irrespective of the

nature of the chain backbone or the absence of it. It could be that the basic structure of these substances is determined primarily by the necessity to maintain a 6 Å contact distance between neighboring phenyls, and the chain backbone is merely disposed to fill the gap left by these phenyls.

In our model, the short range structure arises from the interactions which, aside from the intramolecular constraints such as bond torsional potentials, comprise solely Lennard-Jones type potentials. Yet we were able to reproduce most of the experimental data which reflect the short range structure, including the X-ray scattering pattern[19] and its temperature dependence,[25] the neutron scattering curves of selectively deuterated samples,[20] and the glass transition behavior.[25] Although these agreements do not guarantee that our model is correct in all the details, they nevertheless suggest that the structural features in the length scale of concern here, namely 1 to ~15 Å, are likely to be adequately represented. In the molecular dynamics simulation of benzene,[39] three different potential models, including the one with a point quadrupole at the ring center, were compared. Although the one with the quadrupole appears to give a better agreement for the crystalline benzene structure, no obvious superiority of any one of them over the others can be ascertained in the liquid structure, in which a high probability of benzene–benzene separation at around 6 Å was indicated in all three cases. The high probability of 6 Å separation was also predicted in the RISM model of benzene,[36] in which atoms interact only with repulsive potentials.

In calculating the conformational energy maps of meso and racemic diads of polystyrene, Yoon, Sundararajan, and Flory[30] included only Lennard-Jones potentials in the nonbonded interactions. More recently, Rapold and Suter[31] recalculated the conformational energy maps using a potential energy model that includes electrostatic interactions due to partial charges residing on the atoms. The resulting energy maps showed some differences from the YSF maps and also from our conformer population maps shown in Figures 11 and 12, especially with regard to the depths of the energy minima for the tt and gg conformations of meso diads. However, when they constructed[27] a model of *bulk* amorphous polystyrene by an energy minimization technique and examined the resulting conformers, the population distribution map for the meso diads turned out to resemble our Figure 11 closely (within the statistical uncertainties which are relatively large). The implication is that for a single isolated chain the influence of electrostatic charges on the conformation is fairly large, but in the presence of many other molecules in the bulk state the influence of electrostatic interaction becomes all but negligible in comparison to the overwhelming influence of the repulsive part of the Lennard-Jones interactions.

Summary

A molecular dynamics simulation of bulk atactic polystyrene was performed with a united atom model and an all atom model. In parts 1 and 2 the calculated X-ray and neutron scattering intensity curves were shown to agree much better with experiment when the united rather than the all atom model was used. In this work we analyze the result obtained with the united atom model in detail to determine the short range order present in polystyrene glass. Most of the results presented are with a system in which a molecule of 80 monomers is packed in a cubic MD cell with periodic boundary conditions (to a density of 1.028 g/cm^3). Some limited amount of study was also made with a system containing two molecules of 40 monomers each in an MD cell of the same size. Slightly different methods of separating the *intra-* from the *inter*molecular effects were used in analyzing the results obtained with these two systems. Comparison of the two showed that the basic features of the short range order present were unaffected by the subtle ambiguities in the definition of the *intra-* and *inter*molecular pairs inherent in polymeric systems.

During the study of the *intra*molecular correlation of phenyl group centers, the radial distribution function was evaluated individually according to whether the pair of phenyl groups considered were first neighbors ($m = 1$), second neighbors ($m = 2$), etc., along the contour of the chain. It was seen that some of the second and third neighbor pairs approach each other to distances that were shorter than the distance adopted by first neighbor pairs. This fact suggests that the basic assumption underlying the rotational isomeric states model, that is, the assumption that the "third or higher order" steric interactions can be neglected, may have to be re-examined more closely.

The local chain conformation adopted by the polystyrene molecule was examined by evaluating the population distribution of backbone C–C bond torsional angles (ϕ_i, ϕ_{i+1}) for meso and racemic diads. The resulting contour maps were compared with the conformation energy maps prepared previously by others as a step in formulating the rotational isomeric states model of a polystyrene chain. There are a great deal of similarities, but also some differences. These differences may arise either from the "third and higher order" effect neglected in the rotational isomeric states model or from the effect of *inter*molecular interactions present only in the bulk system. To see which of these is more important, our population distribution maps have to be compared with conformational energy maps derived with exactly the same set of force field parameters as used here.

In the *inter*molecular correlation, the most prominent feature noted was the strong preference for the phenyl groups to be apart by about 6 Å from center to center. To see the mutual orientation of the pair of phenyls at this 6 Å distance, we evaluated the population distribution of the second phenyl located in the direction Θ, Φ with respect to the first phenyl at the origin. The angles Θ and Φ are the spherical polar coordinates of the center of the second phenyl in the system O-*XYZ* where *Z* axis is perpendicular to the first phenyl plane and the *X* axis is in the direction from its center to its *para* carbon atom. The result shows that the population density is concentrated in the region given by $60° < \Theta < 90°$ and $-120° < \Phi < 120°$, and the density maxima are at $\Theta = \sim 75°$ and $\Phi = \sim \pm 25°$.

Integration of the radial distribution function shows that within the first coordination shell of a phenyl group, defined as extending to a radius of 8 Å, there exist 12.3 neighbor phenyl groups altogether, of which about 5.1 are *intra*molecular and 5.5 are *inter*molecular, with the remainder in the unclassified category. Examination of the averaged order parameters describing the mutual orientational correlations of chain backbones shows that, while the *inter*molecular pair of backbones segments tend to line up parallel when the separation between them is less than 5 Å, such occurrences are rare, and for any separations larger than 6 Å the

*inter*molecular backbone pairs are essentially randomly oriented to each other.

The preponderance of 6 Å separation between aromatic rings was previously found in liquid and crystalline benzene and in most crystalline peptides and proteins having phenyl side groups, and the same tendency is found here in amorphous polystyrene. We may speculate that in all these substances the basic structure is determined primarily by the necessity to maintain a 6 Å contact distance between neighboring phenyls, irrespective of the nature of the chain backbone or the absence of it. This 6 Å separation between phenyl centers appears to be dictated by the repulsive part of the nonbonded interatomic interactions.

Acknowledgment. This work was supported in part by the NSF Grant DMR8909232. The computation performed in this work was carried out on the Cray Y-MP/864 at the Ohio Supercomputer Center, and the generous allocation of cpu time is greatly appreciated.

References and Notes

(1) Hansen, J. P.; McDonald, I. R. *Theory of Simple Liquids*, 2nd ed.; Academic Press: New York, 1986.
(2) Kohler, F. *The Liquid State*; Verlag Chemie, Weinheim, Germany, 1972.
(3) Geil, P. H. *J. Macromol. Sci., Phys. Ed.* **1976**, *12*, 173.
(4) Wang, C. S.; Yeh, G. S. Y. *J. Macromol. Sci., Phys. Ed.* **1978**, *15*, 107.
(5) Pechhold, W. R.; Grossmann, H. P. *Faraday Discuss. Chem. Soc.* **1979**, *68*, 58.
(6) Katz, J. R.; Selman, J.; Heyne, L. *Z. Kautschuk* **1927**, 217.
(7) Katz, J. R. *Trans. Faraday Soc.* **1936**, *32*, 77.
(8) Krimm, S. *J. Phys. Chem.* **1953**, *57*, 22.
(9) Bjørnhaug, A.; Ellefsen, Ø.; Tønnesen, B. A. *J. Polym. Sci.* **1954**, *12*, 621.
(10) Kilian, G. G.; Bourke, K. *J. Polym. Sci.* **1962**, *58*, 311.
(11) Wecker, S. M.; Davidson, T.; Cohen, J. B. *J. Mater. Sci.* **1972**, *7*, 1249.
(12) Adams, R.; Balyuzi, H. H.; Burge, R. E. *J. Mater. Sci.* **1978**, *13*, 391.
(13) May, M. *J. Polym. Sci., Polym. Symp.* **1977**, *58*, 23.
(14) Lovell, R.; Windle, A. H. *Polymer* **1976**, *17*, 488.
(15) Lovell, R.; Mitchell, G. R.; Windle, A. H. *Faraday Discuss. Chem. Soc.* **1979**, *68*, 46.
(16) Mitchell, G. R.; Windle, A. H. *Polymer* **1984**, *25*, 906.
(17) Schubach, H. R.; Nagy, E.; Heise, B. *Colloid Polym. Sci.* **1982**, *259*, 789.
(18) Schärpf, O.; Gabrys, B.; Peiffer, D. G. ILL Report No. 90SC26T, Grenoble, France, 1990.
(19) Mondello, M.; Yang, H.-J.; Furuya, H.; Roe, R. J. *Macromolecules* **1994**, *27*, 3566.
(20) Furuya, H.; Mondello, M.; Yang, H.-J.; Roe, R. J.; Erwin, R. W.; Han, C. C.; Smith, S. D. *Macromolecules* **1994**, *27*, 5674.
(21) Williams, W. G. *Polarized Neutrons*; Clarendon Press: Oxford, England, 1988.
(22) Moon, R. N.; Riste, T.; Koehler, W. C. *Phys. Rev.* **1969**, *181*, 920.
(23) Schärpf, O. *Neutron Scattering in the Nineties*; International Atomic Energy Agency: Vienna, Austria, 1985; p 85.
(24) Song, H. H.; Roe, R. J. *Macromolecules* **1987**, *20*, 2723.
(25) Roe, R. J. To be published.
(26) Johnson, L. F.; Heatley, F.; Bovey, F. A. *Macromolecules* **1970**, *3*, 175.
(27) Rapold, R.; Suter, U. W.; Theodorou, D. N. *Makromol. Chem. Theory Simul.* **1994**, *3*, 19.
(28) Flory, P. J. *Statistical Mechanics of Chain Molecules*; Hanser: New York, 1969.
(29) Flory, P. J.; Sundararajan, P. R.; DeBolt, L. C. *J. Am. Chem. Soc.* **1974**, *96*, 5015.
(30) Yoon, D. Y.; Sundararajan, P. R.; Flory, P. J. *Macromolecules* **1975**, *8*, 776.
(31) Rapold, R.; Suter, U. W. *Makromol. Chem. Theory Simul.* **1994**, *3*, 1.
(32) Abe, Y.; Tonelli, A. E.; Flory, P. J. *Macromolecules* **1970**, *3*, 294.
(33) Tonelli, A. E. *Macromolecules* **1973**, *6*, 683.
(34) Narten, A. H. *J. Chem. Phys.* **1968**, *48*, 1630.
(35) Lowden, L. J.; Chandler, D. *J. Chem. Phys.* **1974**, *61*, 5228.
(36) Narten, A. H. *J. Chem. Phys.* **1977**, *67*, 2102.
(37) Cox, E. G.; Cruickshank, D. W. J.; Smith, J. A. S. *Proc. R. Soc. London* **1958**, *247A*, 1.
(38) Burley, S. K.; Petsko, G. A. *J. Am. Chem. Soc.* **1986**, *108*, 7995.
(39) Claessens, M.; Ferrario, M.; Ryckaert, J.-P. *Mol. Phys.* **1983**, *50*, 217.

MA9460089